Synthesis and EPR studies of the first water-soluble N@C_{60} derivative

Stuart P. Cornes[a], Shen Zhou[a] and Kyriakos Porfyrakis[a]*

[a] *Department of Materials, University of Oxford, 16 Parks Road, Oxford, OX1 3PH, UK. Email: kyriakos.porfyrakis@materials.ox.ac.uk; Tel.: +44(0)1865 273724.*

The first water-soluble derivative of the paramagnetic endohedral fullerene N@C_{60} has been prepared through the covalent attachment of a single addend containing two permethylated β-cyclodextrin units to the surface of the carbon cage. The line width of the derivatives EPR signal is highly sensitive to both the nature of the solvent and the presence of Cu(II) ions in solution.

N@C_{60} is a paramagnetic endohedral fullerene species comprised of a single nitrogen atom incarcerated within a C_{60} fullerene cage. As the nitrogen is shielded from the external environment, N@C_{60} has extremely long spin relaxation times (T_1 = 0.375 ms, T_2 = 0.25 ms).[1] For this reason, it has been proposed as a promising building block for a quantum information processing device.[2–4] The long relaxation rates also provide the molecule with a very sharp EPR signal that is highly sensitive to interactions with other paramagnetic species.[5,6] Recent work in our group has shown that a substantial broadening of the signal occurs in an N@C_{60}-copper-phthalocyanine dyad system, which is caused by a dipolar coupling interaction between the nitrogen and copper spin centres.[7] This suggests that N@C_{60} may also find applications as a spin probe.

The vast majority of spin probes currently used are either nitroxide- or trityl-based radicals, with water-soluble derivatives of these used for an array of biological applications such as oximetry measurements[8–11] and distance measurements in biomolecules.[12,13] In order to investigate if N@C_{60} could be used in such a capacity it is necessary for the inherently hydrophobic fullerene cage to be functionalised with hydrophilic groups to render it compatible with aqueous environments. Several methods for the solubilisation of empty cage and other endohedral fullerenes have been demonstrated.[14–20] However, many of these methods are unsuitable for the solubilisation of N@C_{60}, as loss of the nitrogen atom has been shown to occur when the fullerene is exposed to harsh reaction conditions, such as prolonged heating or addition of large quantities of base.[21–23] We have recently reported an adaptation of the widely used Bingel reaction, in which minimal loss of nitrogen occurred[23] and hence we aimed to utilise this reaction protocol to prepare the first water-soluble N@C_{60} derivative. The attachment of addends containing permethylated cyclodextrin units is a highly effective method of solubilising C_{60}.[24–30] We therefore chose to use a symmetric malonate derivative containing two primary-rim functionalised permethylated-β-cyclodextrin units in the functionalisation of N@C_{60}.

Synthesis of the target malonate is shown in Scheme 1.[28] Alcohol **1**[31] was initially condensed with malonyl dichloride to give bis-ester **2**. Deprotection of the *tert*-butyl ester groups with TFA afforded bis-acid **3** which was subsequently reacted

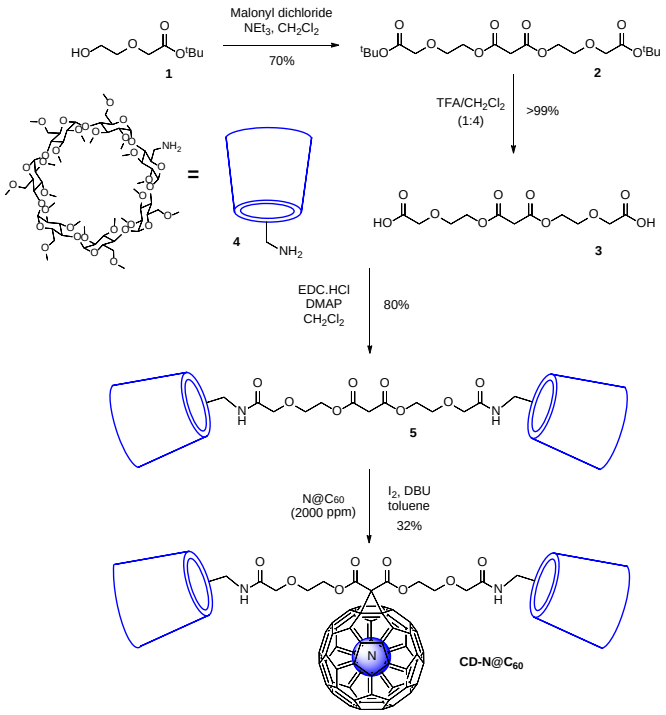

Scheme 1: Synthesis of N@C_{60} derivative **CD-N@C_{60}**.

with 6^{A}-amino-permethylated β-cyclodextrin **4**[32,33] under EDC coupling conditions to give the the desired material **5**. The malonate was reacted with a 0.2% purity sample of N@C_{60}/C_{60} under our modified, spin-compatible, Bingel reaction conditions, in which the base (DBU) was added in a dilute toluene solution rather than directly.[23] The crude material was then purified using preparative thin layer chromatography to afford derivative **CD-N@C_{60}** in a 32% yield as a red-brown solid (Scheme 1). Quantitative electron paramagnetic resonance (EPR) measurements revealed that the spin concentration of the product was 82% of that of the starting material. This is in line with the spin retention levels previously documented for this reaction protocol. Importantly, **CD-N@C_{60}** is highly soluble in water (~ 200 mg/mL) as well as a range of organic solvents including toluene, dichloromethane, chloroform, acetone, ethyl acetate and methanol.

MALDI mass spectrometry was performed on **CD-N@C_{60}**, which showed the expected molecular ion peak for the empty cage derivative but no peak for the endohedral species (ESI, Figure S8). This is unsurprising considering the low N@C_{60} content of the starting material. A larger amount of the pure empty cage analogue (**CD-C_{60}**) was also prepared so that ^{1}H and ^{13}C NMR characterisation of the adduct could be undertaken (see ESI).

In order to confirm the presence of the endohedral nitrogen in **CD-N@C_{60}**, an X-band continuous wave electron paramagnetic resonance (cw-EPR) spectrum was acquired in toluene at room temperature, which showed the expected spin signal for the N@C_{60} moiety (ESI, Figure S9). Due to rapid tumbling of **CD-N@C_{60}** in solution the spectrum appears the same as that of pristine N@C_{60}, in which the nitrogen spin is in a highly isotropic environment and produces three sharp lines due to a hyperfine coupling interaction with the ^{14}N nuclear spin (I = 1). An Easyspin fit[34] of the data revealed the line shape to be purely Lorentzian in character, with a peak-to-peak line width (LW_{pp}) of 6.0 μT. This is substantially broader than the T_2 derived line width calculated for pristine N@C_{60} (< 0.3 μT).[1] A major contribution to the homogeneous broadening observed comes from a fluctuating zero field splitting (ZFS) interaction generated through the functionalisation of the cage, which is known to reduce the relaxation rate of the nitrogen electron spin.[35] Additionally, there may be small contributions from inhomogeneous broadening mechanisms related to the instrument used, such as inhomogeneities in its external magnetic field[36] and the high modulation frequency (100 kHz) used for the measurements.[37]

To directly observe the ZFS generated through functionalisation of the cage, a solid-state cw-EPR spectrum (toluene, 100 K) of the product was also collected (Figure 1). This showed additional peaks indicative of a ZFS interaction caused by the reduction in the symmetry of the C_{60} cage. Fitting of the data using an Easyspin simulation[34] afforded the isotropic g-factor and hyperfine coupling constant (g = 2.00263, A_{iso} = 15.77 MHz), and the characteristic ZFS parameters (D = 8.72, E = 0.57 MHz) which are all consistent with those determined for other mono-functionalised N@C_{60} derivatives prepared *via* Bingel reaction.[23,38]

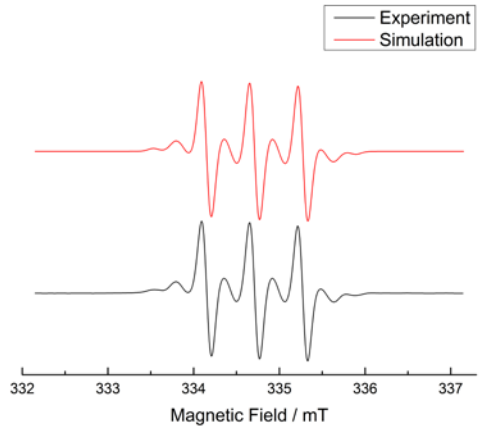

Figure 1: X-band cw-EPR spectrum of **CD-N@C_{60}** (toluene, 100 K); experimental data (black line), Easyspin simulation (red line).

A solution-state spectrum of **CD-N@C_{60}** was also obtained in aqueous media (Figure 2). This again showed the expected three lines, however the signal was significantly broader (19.1 μT) and the line shape was found to have both Lorentzian and Gaussian components. The Lorentzian component of the LW_{pp} is approximately two times larger than the LW_{pp} obtained in toluene (12.7 μT vs. 6.0 μT), indicating an even faster spin relaxation rate in this solvent. T_2 is inversely proportional to the both the square of the effective ZFS parameter (D_{eff}; $D_{eff}^2 = D^2 + 3E^2$) and the rotational correlation time (τ_C) of the molecule.[1] However, a solid-state spectrum of **CD-N@C_{60}** in water (ESI, Figure S10) showed an identical set of ZFS parameters to that of the frozen toluene solution, suggesting the change in line width is purely caused by a reduction in τ_C. The decrease in the rate of tumbling of **CD-N@C_{60}** in aqueous media is most likely a consequence of agglomeration of the compound due to its amphiphilic nature. Indeed, aggregation of **CD-C_{60}** has previously been noted, with evidence provided by a substantial broadening of its ^{1}H NMR spectrum in D_2O and the lack of a peak at ~430 nm in the UV-vis spectrum.[28] The inhomogeneous or Gaussian component of the broadening (11.3 μT contribution to LW_{pp}) in water, is potentially due to intermolecular dipolar interactions between N@C_{60} units within the same cluster, however further experiments are needed to verify this.

Next, we investigated the ability of **CD-N@C_{60}** to function as a spin-probe in aqueous media. It has previously been shown that both T_1 and T_2 relaxation rates of pristine N@C_{60} have a linear dependence on the concentration of other paramagnetic species, such as the nitroxide radical TEMPO, in toluene.[39] This is the result of an intermolecular dipolar coupling interaction between the electron spin of the two species, which can be expressed as:

$$\Delta T_1^{-1} \propto \frac{D\gamma_X \hbar S_{(X)}\left(S_{(X)}+1\right)}{\omega^2 r_0^5}[X^{\cdot}]$$

where D is the diffusion coefficient of the species X, γ_X is the gyromagnetic ratio of X, ω is the electronic Larmor frequency and r_0 is the distance of closest approach of the two spins. As the LW_{pp} of the N@C_{60} signal is inversely proportional to the

relaxation time T_2, we decided to see how the line width of an aqueous solution of **CD-N@C$_{60}$** was affected by the addition of Cu(II) ions (added as $CuSO_4$). Interestingly, no broadening of the signal was observed even at a very high Cu(II) concentration (0.5 M). This suggests that the aggregates of **CD-N@C$_{60}$** formed in water have a micellar structure with a hydrophilic shell of cyclodextrin units shielding the hydrophobic C_{60} cages from the solvent. As there is no driving force for the Cu(II) ions to penetrate through this shell this results in a large distance of closest approach of the nitrogen and copper spins and therefore a very small dipolar coupling interaction between them, which cannot be detected through a change in line width.

To confirm this the measurements were repeated in acetone, a solvent in which no aggregation was expected to occur§. In this case it was anticipated that direct collisions between the C_{60} cage and the Cu(II) ions could occur, resulting in a significantly shorter distance of closest approach of the two spins and hence a much larger dipolar coupling interaction§§. Indeed, the line width was found to increase linearly in a 1 – 100 mM Cu(II) concentration range, with a sensitivity of 2.6 µT/mM (Table 1 and Figure 3). The limit of detection (LOD) was calculated to be 110 µM§§§.[40] At this concentration, it is only possible to directly observe the copper EPR signal if a large modulation amplitude is applied to the measurement (ESI, Figure S13), highlighting the utility of this probe. Whilst this LOD is significantly higher than those determined for optical[41] and electrochemical[42] based Cu(II) sensors (LOD < 0.1 µM) it should be possible to reduce the LOD with **CD-N@C$_{60}$** if an instrument with improved field homogeneity that can provide a lower modulation frequency is used.

Table 1: Peak-to-peak line widths measured for acetone solutions of **CD-N@C$_{60}$** containing different concentrations of Cu(II) ions (298 K).

[Cu(II)] (mM)[a]	ΔLW_{pp} (µT) acetone	ΔLW_{pp} (µT) EtOH
0	0	0
1	2.4	1.1
10	31.0	7.7
100	258.9	81.6

[a]$Cu(ClO_4)_2{\cdot}6H_2O$ used as source of Cu(II).

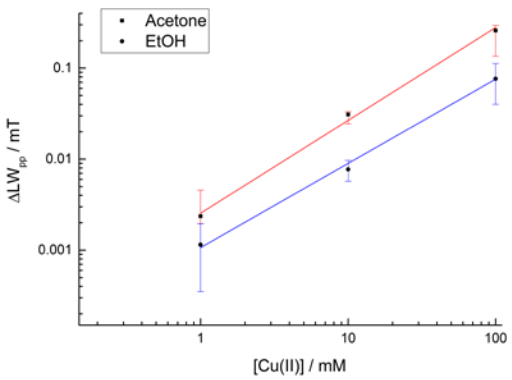

Figure 3: Plot of the change in peak-to-peak line width against Cu(II) ion concentration in acetone (squares, red line) and ethanol (circles, blue line).

It also proved possible for detection to occur in ethanol over the same concentration range (Table 1, Figure 3), however the sensitivity of the probe was reduced to 0.8 µT/mM and the LOD increased to 280 µM, in this solvent. As ethanol has a polarity that is intermediate of acetone and water it may be that partial aggregation of **CD-N@C$_{60}$** is occurring, which would result in a lower collision frequency between the cage and the Cu(II) ions, and hence a reduced broadening effect.

To further investigate the aggregation of the system, dynamic light scattering (DLS) measurements of the empty cage derivative were conducted in both water and acetone solution. From the number-weighted size distribution profiles displayed in Figure 4, small aggregates with a diameter of approximately 4.5 nm are seen in the water sample. As already stated, it is likely that these aggregates have a micellar structure, with their size limited due to the short length of the linker between the fullerene and the sterically bulky cyclodextrin units. Indeed, a dendritic fullerene amphiphile, reported by Hirsch and co-workers, was also observed to form micellar aggregates of a similar size by cryogenic transmission electron microscopy.[43] In stark contrast, a particle size of 1.5 nm was seen in the acetone sample suggesting complete dispersion of **CD-C$_{60}$** in this solvent, as expected.

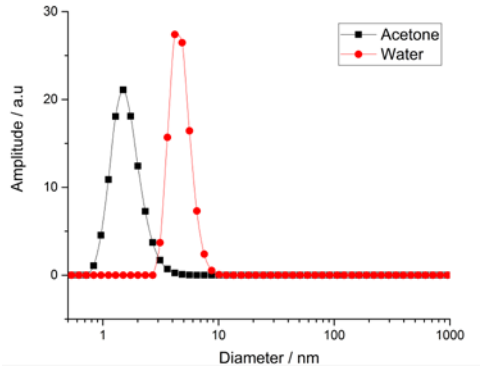

Figure 4: Number-weighted size distribution profile of **CD-N@C$_{60}$** in water (red) and acetone (black) (T = 298 K).

In summary, the first example of a water-soluble derivative of N@C_{60} has been prepared and its EPR signal measured in aqueous media. The derivative was shown to act as an effective spin-probe for Cu(II) ions in polar organic solvents. It should be noted that the sensitivity of **CD-N@C$_{60}$** is approximately four orders of magnitude lower than the sensitivity observed with typical nitroxide-based spin sensors.[44] This is a consequence of the lack of a Heisenberg exchange component to the interaction, which is purely dipolar in nature, and suggests that an N@C_{60} spin probe that relies solely on collisions between the fullerene cage and the paramagnetic analyte may have limited utility. To improve sensitivity it may be necessary to attach a binding site to the surface of the fullerene that would hold the analyte at a fixed short distance from the nitrogen spin center. Such a system should have both improved sensitivity and a lower LOD. Additionaly, adaptation of the design of the system to prevent aggregation may allow for its use as a probe for the detection

of paramagnetic species in a biological environment. In particular, we are targeting the use of N@C_{60} as an oximetry probe. This will be the subject of a future publication.

We thank Prof. Paul Beer from the Univeristy of Oxford for useful discussions and use of equipment. We thank The Centre for Advanced Electron Spin Resonance (CAESR) for use of ESR instruments. SZ thanks the National University of Defence Technology and Prof. Haifeng Cheng for a studentship and support. We acknowledge EPRSC funding for the Fellowship programme 'Manufacturing the future: endohedral fullerenes, small molecules, big challenges' (EP/K030108/1).

Conflicts of Interest

There are no conflicts of interest to declare.

Notes and references

§ $Cu(ClO_4)_2{\cdot}(H_2O)_6$ used as source of Cu(II) ions for acetone experiments.
§§ The ESR signal for the copper spin is identical in the absence and presence of **CD-N@C_{60}** suggesting that the Cu(II) ions do not coordinate with the cyclodextrin units (ESI, Figure S14).
§§§ Calculated using the expression: LOD = 3σ/k, where σ is the standard error in the measurement of the linewidth of **CD-N@C_{60}** in the absence of Cu(II) and k is the gradient of the linear plot.[40]

1 J. J. L. Morton, A. M. Tyryshkin, A. Ardavan, K. Porfyrakis, S. A. Lyon and G. Andrew D. Briggs, *J. Chem. Phys.*, 2006, **124**, 014508.
2 W. Harneit, *Phys. Rev. A*, 2002, **65**, 032322.
3 S. C. Benjamin, A. Ardavan, G. A. D. Briggs, D. A. Britz, D. Gunlycke, J. Jefferson, M. A. G. Jones, D. F. Leigh, B. W. Lovett, A. N. Khlobystov, S. A. Lyon, J. J. L. Morton, Kyriakos Porfyrakis, M. R. Sambrook and A. M. Tyryshkin, *J. Phys. Condens. Matter*, 2006, **18**, S867.
4 W. L. Yang, Z. Y. Xu, H. Wei, M. Feng and D. Suter, *Phys. Rev. A*, 2010, **81**, 032303.
5 G. Liu, A. N. Khlobystov, G. Charalambidis, A. G. Coutsolelos, G. A. D. Briggs and K. Porfyrakis, *J. Am. Chem. Soc.*, 2012, **134**, 1938–1941.
6 B. J. Farrington, M. Jevric, G. A. Rance, A. Ardavan, A. N. Khlobystov, G. a. D. Briggs and K. Porfyrakis, *Angew. Chem. Int. Ed.*, 2012, **51**, 3587–3590.
7 S. Zhou, M. Yamamoto, G. A. D. Briggs, H. Imahori and K. Porfyrakis, *J. Am. Chem. Soc.*, 2016, **138**, 1313–1319.
8 A. Bratasz, A. C. Kulkarni and P. Kuppusamy, *Biophys. J.*, 2007, **92**, 2918–2925.
9 R. Ahmad and P. Kuppusamy, *Chem. Rev.*, 2010, **110**, 3212–3236.
10 S. R. Burks, J. Bakhshai, M. A. Makowsky, S. Muralidharan, P. Tsai, G. M. Rosen and J. P. Y. Kao, *J. Org. Chem.*, 2010, **75**, 6463–6467.
11 J. Frank, M. Elewa, M. M. Said, H. A. El Shihawy, M. El-Sadek, D. Müller, A. Meister, G. Hause, S. Drescher, H. Metz, P. Imming and K. Mäder, *J. Org. Chem.*, 2015, **80**, 6754–6766.
12 V. Meyer, M. A. Swanson, L. J. Clouston, P. J. Boratyński, R. A. Stein, H. S. Mchaourab, A. Rajca, S. S. Eaton and G. R. Eaton, *Biophys. J.*, 2015, **108**, 1213–1219.
13 J. J. Jassoy, A. Berndhäuser, F. Duthie, S. P. Kühn, G. Hagelueken and O. Schiemann, *Angew. Chem. Int. Ed.*, 2017, **56**, 177–181.
14 J. Li, A. Takeuchi, M. Ozawa, X. Li, K. Saigo and K. Kitazawa, *J. Chem. Soc. Chem. Commun.*, 1993, **0**, 1784–1785.
15 M. Brettreich and A. Hirsch, *Tetrahedron Lett.*, 1998, **39**, 2731–2734.
16 S. Oriana, S. Aroua, J. O. B. Söllner, X.-J. Ma, Y. Iwamoto and Y. Yamakoshi, *Chem. Commun.*, 2013, **49**, 9302–9304.
17 M. Wang, L. Huang, S. K. Sharma, S. Jeon, S. Thota, F. F. Sperandio, S. Nayka, J. Chang, M. R. Hamblin and L. Y. Chiang, *J. Med. Chem.*, 2012, **55**, 4274–4285.
18 I. Nierengarten and J.-F. Nierengarten, *Chem. – Asian J.*, 2014, **9**, 1436–1444.
19 I. Rašović, *Mater. Sci. Technol.*, 2016, **0**, 1–18.
20 T. Li and H. C. Dorn, *Small*, 2017, **13**, 1603152.
21 A. Iwasiewicz-Wabnig, K. Porfyrakis, G. A. D. Briggs and B. Sundqvist, *Phys. Status Solidi B*, 2009, **246**, 2767–2770.
22 G. Liu, A. N. Khlobystov, A. Ardavan, G. A. D. Briggs and K. Porfyrakis, *Chem. Phys. Lett.*, 2011, **508**, 187–190.
23 S. Zhou, I. Rašović, G. A. D. Briggs and K. Porfyrakis, *Chem. Commun.*, 2015, **51**, 7096–7099.
24 S. Filippone, F. Heimann and A. Rassat, *Chem. Commun.*, 2002, 1508–1509.
25 Y. Liu, Y.-L. Zhao, Y. Chen, P. Liang and L. Li, *Tetrahedron Lett.*, 2005, **46**, 2507–2511.
26 S. Xiao, Q. Wang, F. Yu, Y. Peng, M. Yang, M. Sollogoub, P. Sinaÿ, Y. Zhang, L. Zhang and D. Zhou, *Bioorg. Med. Chem.*, 2012, **20**, 5616–5622.
27 F. Giacalone, F. D'Anna, R. Giacalone, M. Gruttadauria, S. Riela and R. Noto, *Tetrahedron Lett.*, 2006, **47**, 8105–8108.
28 S. Filippone and A. Rassat, *Comptes Rendus Chim.*, 2003, **6**, 83–86.
29 Z. Guan, Y. Wang, Y. Chen, L. Zhang and Y. Zhang, *Tetrahedron*, 2009, **65**, 1125–1129.
30 J. Yang, Y. Wang, A. Rassat, Y. Zhang and P. Sinaÿ, *Tetrahedron*, 2004, **60**, 12163–12168.
31 X. Zhang, X. Du, X. Huang and Z. Lv, *J. Am. Chem. Soc.*, 2013, **135**, 9248–9251.
32 N. Zhong, H.-S. Byun and R. Bittman, *Tetrahedron Lett.*, 1998, **39**, 2919–2920.
33 P. J. Skinner, A. Beeby, R. S. Dickins, D. Parker, S. Aime and M. Botta, *J. Chem. Soc. Perkin Trans. 2*, 2000, 1329–1338.
34 S. Stoll and A. Schweiger, *J. Magn. Reson.*, 2006, **178**, 42–55.
35 J. Zhang, J. J. L. Morton, M. R. Sambrook, K. Porfyrakis, A. Ardavan and G. A. D. Briggs, *Chem. Phys. Lett.*, 2006, **432**, 523–527.
36 J. A. Weil and J. R. Bolton, *Electron paramagnetic resonance: elementary theory and practical applications*, John Wiley & Sons, 2007.
37 J. J. L. Morton, A. M. Tyryshkin, A. Ardavan, K. Porfyrakis, S. A. Lyon and G. A. D. Briggs, *J. Chem. Phys.*, 2005, **122**, 174504.
38 K. Lips, M. Waiblinger, B. Pietzak and A. Weidinger, *Phys. Status Solidi A*, 2000, **177**, 81–91.
39 K.-P. Dinse, in *Electron Paramagnetic Resonance: Volume 17*, eds. B. C. Gilbert, M. J. Davies and K. A. McLauchlan, The Royal Society of Chemistry, 2000, vol. 17, pp. 78–108.
40 X. Wei, Z. Zhou, T. Hao, H. Li, Y. Xu, K. Lu, Y. Wu, J. Dai, J. Pan and Y. Yan, *Anal. Chim. Acta*, 2015, **870**, 83–91.
41 X. Liu and Y. Zhang, *J. Fluoresc.*, 2016, **26**, 2267–2270.
42 S. Yang, B. Xia, X. Zeng, S. Luo, W. Wei and X. Liu, *Anal. Chim. Acta*, 2010, **667**, 57–62.
43 S. Burghardt, A. Hirsch, B. Schade, K. Ludwig and C. Böttcher, *Angew. Chem. Int. Ed.*, 2005, **44**, 2976–2979.
44 A. J. Hoff, *Advanced EPR: applications in biology and biochemistry*, Elsevier, 2012.